Science & Technology Development Journal, 24(SI1):SI51-SI62

Open Access Full Text Article

Research Article

Interaction of curcumin molecule with fullerene material by simulation method

Le Vu Phuc[1,2], Lam Toan Vi[1,2], Tran Thi Thu Hanh[1,2,*]

Use your smartphone to scan this QR code and download this article

ABSTRACT

The designs of target-drug delivery systems are attractively concerned due to their efficacy and safety. Fullerene is the first symmetrical carbon nanomaterial invented in the world. Due to the special properties of fullerene, it is an emergent topic in nanomaterials in recent years. Many experimental studies used this material to form the drug-carrier system and have shown a significant improvement in the pharmacokinetic properties of the active substance. Curcumin is a natural compound extracted from turmeric, with many pharmacological properties such as antiviral, antibacterial, and impact on cancer cells, etc. However, curcumin's pharmacological properties are hardly clinically demonstrated due to its water-solubility. A fullereo-curcuminoid derivative to HIV viruses and cancer cells was created, in which curcumin is out-bound to fullerene. HIV antiviral properties showed only moderate efficiency, and no anti-cancer effect was observed. Another disadvantage of the out-bound fullereo-curcuminoid derivative is that it is hard to control the number of curcumin-derivative molecules that bind out-surfaced fullerene, which is a critical problem we need to deal with since curcumin overdose causes side effects to the digestive system, skin, or headache. For the above reasons, we decided to conduct this research, focusing on the computational approach of in-bound fullereo-curcuminoid derivative systems for drug delivery, with adequate fullerene size to encapsulate curcumin molecules. This proposed model is promising not only to create a better anti-solvent shield for the curcumin molecule throughout the delivery path to the target cells but also to manipulate the curcumin dose since the fullerene shield may increase the efficiency of curcumin carrying. This research uses the computational simulation method to investigate the epidermal growth factor (EGF) receptor binding and the physicochemical parameters of the curcumin molecule encapsulated in fullerene. The density functional theory (DFT) calculation is conducted to observe the electrical and energetic properties of the curcumin-fullerene encapsulation system. The obtained system is then docked with the target receptor. After that, the size-modified defected gap will be created on the fullerene surface in the release process of the curcumin out of the fullerene. To interact with the target residues on the receptor will be observed by using MD simulation and their interaction stabilization.

Key words: Curcumin, Drug delivery design, Fullerene-based drug delivery, In-silico

[1]*Laboratory of Computational Physics, Faculty of Applied Science, Ho Chi Minh City University of Technology (HCMUT), Ho Chi Minh City, 268 Ly Thuong Kiet Street, District 10, Ho Chi Minh City, Viet Nam*

[2]*Vietnam National University Ho Chi Minh City, Linh Trung Ward, Thu Duc District, Ho Chi Minh City, Viet Nam*

Correspondence

Tran Thi Thu Hanh, Laboratory of Computational Physics, Faculty of Applied Science, Ho Chi Minh City University of Technology (HCMUT), Ho Chi Minh City, 268 Ly Thuong Kiet Street, District 10, Ho Chi Minh City, Viet Nam

Vietnam National University Ho Chi Minh City, Linh Trung Ward, Thu Duc District, Ho Chi Minh City, Viet Nam

Email: thuhanhsp@gmail.com

History

- Received: 2021-09-07
- Accepted: 2021-12-13
- Published: 2022-02-28

DOI : 10.32508/stdj.v24iSI1.3821

Check for updates

INTRODUCTION

Drugs are small organic molecules that are long widely used in health care and medicine. The design of the molecular drug formulas is increasingly applied with advanced techniques to help quickly develop new products that enhance the effectiveness and safety of the treatment process. Along with this development, it is recognized that even drugs developed with the most advanced molecular biology strategies present unacceptable side effects due to their interactions with their non-targets. These effects limit the ability of the medicinal design products to treat diseases such as cancer, neurodegenerative diseases, and other chronic diseases. To handle these issues, new delivery systems such as targeted delivery systems or special control systems need to be designed to help improve efficacy and safety compared to traditional methods[1]. Fullerene or buckyball is a molecule containing 60 carbon atoms (C60). Before that, scientists only knew of two pure forms of carbon: diamond and graphite. In 1985, British chemist Harry Kroto, thanks to a telescope, discovered strange chains of carbon atoms billions of kilometers (km) away in the universe, around massive stars that emit red light. Kroto then had contacts with Richard Smalley and Robert Curl, two American scientists working in short-lived groups of atoms. They used a powerful laser beam to vaporize graphite in helium gas (simulating conditions in red stars) and discovered many previously unknown carbon molecules, most notably C60. The outer shape resembles a soccer ball, and scientists call it a fullerene[2]. The invention, published in the Nature journal, has shocked the scientific world. People quickly realized that fullerene could be a molecule

Cite this article : Phuc L V, Vi L T, Hanh T T T. **Interaction of curcumin molecule with fullerene material by simulation method**. *Sci. Tech. Dev. J.;* 24(SI1):SI51-SI62.

with many very useful applications. In 1996, Curl, Kroto, and Smalley were awarded the Nobel Prize for discovering fullerene. Fullerenes are spherical caged carbon molecules, about 7-30 Å in diameter, consisting of several five-membered (pentagonal) and hexagonal (hexagonal) rings.

Currently, scientists have discovered hundreds of different combinations of hexagons/pentagons. To create a closed cage, all fullerene molecules have the formula of C20 + m, where m is an integer. For example, the proposed structure of C60 is a "truncated icosahedron". A truncated icosahedron is derived by replacing twelve vertices with the five-sided rings. Also, transform the twenty triangle faces with a hexagon ring like a soccer ball with 12 pentagons and 20 hexagons (Figure 1)[3]. Many hollow nested structures can be built using different combinations of hexagons/pentagons. Interestingly, each hollow nested structure contains exactly 12 pentagons, while the number of hexagons is arbitrary. This number of pentagonal rings is required to form a closed hollow cage[4]. The smallest possible fullerene is C20, containing 12 pentagons and no hexagons. Characterizing the bonds in C60, each vertex of the truncated icosahedron is occupied by one carbon atom. Each carbon atom forms a bond with three other carbon atoms, including one double bond and two single bonds[5].

There are two types of roundabouts: (6.6) - Figure 2a and (5,6) - Figure 2b. The connection between two rings of 6 has an average length of 1.391 Å, while the connection between rings of 5 and of 6 has an average length of 1.449 Å[6,7]. Therefore, the bond in the ring bridge (6.6) has similar characteristics to the double bond, while the bond in the ring bridge (5,6) has characteristics close to the single bond. The pentagonal rings have no common sides (Figure 2).

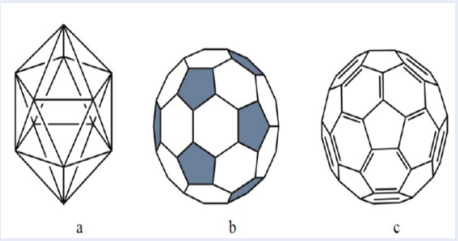

Figure 1: a) Icosahedron; b) Truncated icosahedron; c) Fullerenes, C60[5]. **(Hình này nên có tên chung cho 3 hình thành phần; sau đó chú thích từng thành phần)**

The carbon atoms are in the sp^2 hybridized state (1 hybrid 2s orbital with 2p orbitals) because three sigma bonds are formed with three neighboring carbon atoms, and the other 2p orbital forms pi bonds. The angle between the p axis and the C-C bond vector (θ_p) is 101.6^o[8]. For sp^2 hybridized C atom (trigonal shape), the hybridized orbitals lie in the same plane and have the angle $\theta_p = 0^o$, while for sp^3 hybridized C atom (tetrahedral form), the angle $\theta p = 19.5^o$ (Figure 3). Therefore, the C atom in fullerene (C60) has a geometry closer to the tetrahedral structure than the triangular one.

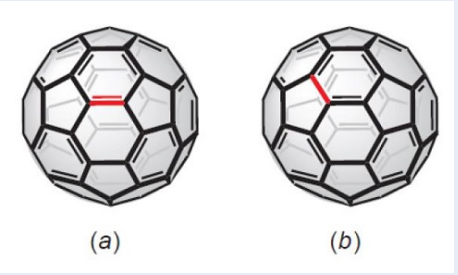

Figure 2: The structure of C60: a) Bond at the ring bridge (6.6); b) Bond at the ring bridge (5,6)[6].

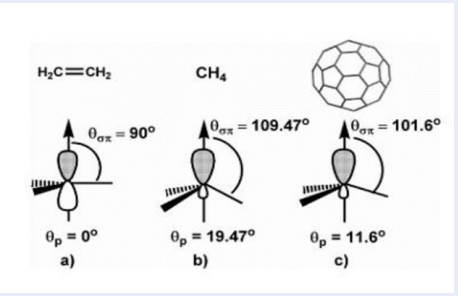

Figure 3: The pyramidal angle ($\theta_p = (\theta_{\sigma\pi} - 90^0)$ of: a) C planar sp^2 hybridization; b) C sp^3 tetrahedral hybrid and c) C sp^2 non-planar hybrid[8].

Fullerene is the world's first symmetric carbon nanomaterial invented. Due to the special properties of fullerenes, it is currently a prominent topic in many areas of nanomaterial research. There have been many experimental studies using this material to form a drug carrier system and have shown a significant improvement in the pharmacokinetic properties of the active substance[9,10]. Curcumin is a natural compound extracted from turmeric, which has many pharmacological properties such as antiviral, antibacterial, anti-cancer. However, due to the insoluble nature of curcumin, the pharmacokinetics of curcumin are hardly observed in clinical studies.

Currently, there are quite a few studies on the construction and simulation of drug delivery system models by using computational methods. For example, research in the field of medicine often focuses on the purification of active ingredients and investigating the effects of the curcumin on the acetylcholinesterase (AChE) and the beta-secretase (BACE-1) receptors loke the work of the authors Thai Khac Minh *et al.*[11]. For fullerenes, there are also some computational simulation studies such as the structure, the antioxidant capacity of some polyphenols, and fullerene derivatives (C60) by using the computational chemistry method by Nguyen Minh Thong[12]. Castro E. Cerón and colleagues conducted an experimental study to create externally bound to fullerenes[10]. Although, as we can see in Figure 4, the fullerene derivative with curcumin by Castro E. Cerón et al.[10], the curcumin molecule binds outside the surface of the fullerene. This makes curcumin more easily exposed to and destroyed by external factors.

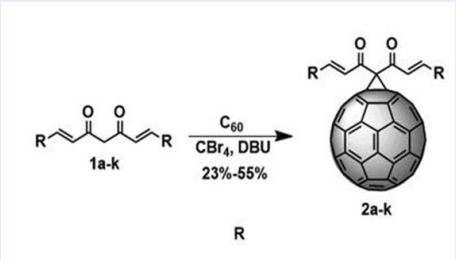

Figure 4: Curcumin and fullerene derivatives by experimental method[10].

The compound in Figure 4 is then tested in vitro for its anti-HIV and anti-cancer effects. The obtained results at a concentration of 3 μM above the derivative could inhibit 64% of HIV infection and help prevent viral entry; however, the antitumor effect was not observed in the group's experiment research[10].

Research on the effect of the curcumin on the tyrosine kinase receptors by the authors A. Golonko, H. Lewandowka, and colleagues has confirmed the role of the curcumin's anti-cancer effect on the different types of cancer. This is an activity commonly found in the polyphenols such as curcumin at the cellular level.

The effects of curcumin are multidirectional on the multiple cancer-suppressive signaling pathways, making it difficult to resist the resistance. At the same time, because it comes from nature, curcumin promises to lead to safe treatment and fewer side effects during the treatment compared to the other cancer chemotherapeutic compounds.

However, due to the curcumin's hydrophobic nature, the curcumin's pharmacokinetic properties cannot be clinically expressed. Many studies are conducted to modify the curcumin molecule to increase the bioavailability properties of this potential molecule[13]. Regarding the simulation calculation method, intending to find the carrier for the active ingredient hydroxyurea (HU), the authors Peng Wang, Ge Yan, Xiaodong Zhu, Yingying Du, Da Chen, and Jinjuan Zhang used a paltry calculation method of the density functional theory (DFT) on two models of the primary fullerene C60 and the fullerene with the MC59 allergens (M=B, Si, Al). The calculated results show that the absorption of the HU on the C60 fullerene is not good and unsuitable as a carrier for the HU (Figure 5). In contrast, the HU is well absorbed on the BC59, the SiC59, and the AlC59, which are potential candidates for the HU distribution system (Figure 6)[14].

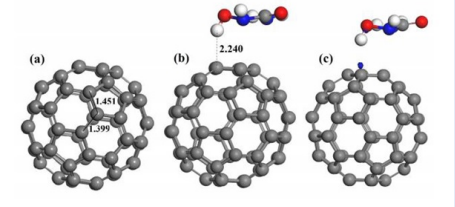

Figure 5: Optimum structures of C60 (a) and HU-C60 (b)[14].

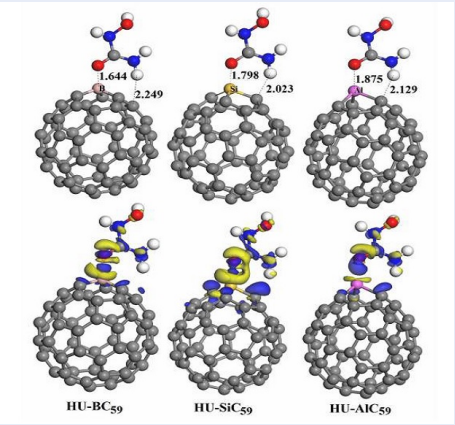

Figure 6: The optimized most stable structures and the corresponding charge density difference (CDD) of HU-BC59, HU-SiC59 and HU-AlC59[14].

To increase the bioavailability of the curcumin, some studies create a derivative of the curcumin with a

fullerene, in which the curcumin is bound to the surface of the fullerene; the derivative is then studied for antivirus effects on HIV and anti-cancer properties [10]. However, the antiretroviral properties of HIV showed an undesirable effect, and no antitumor effects were observed [10]. This can be conjectured that fullerene binds externally to curcumin resulted in the curcumin molecules being degraded on the route of drug delivery. One disadvantage of this derivative is that it is difficult to control the number of the curcumin derivatives that bind to the fullerene, which is a matter of concern because an overdose of the curcumin will cause adverse side effects on the digestive system, skin, or nervous system [15–17]. A model that poses the curcumin inside a fullerene material, meaning that the curcumin is encapsulated with a fullerene molecule, would solve the above problems. Fullerene now could be considered as a new targeted drug carrier. However, the effectiveness of this model has not yet been evaluated, leading to the need for preliminary studies to theoretically evaluate the effectiveness and feasibility of this derived system.

COMPUTATIONAL METHOD

Molecular Structural Data

The structures of the curcumin and the protein Epidermal growth factor receptor (EGFR) are obtained from the database [18] and the protein databank [19], corresponding. The fullerene's model of 540 carbon is built with the Avogadro software.

Molecular dynamic simulation

The curcumin-encapsulated fullerene system, the fullerene defect systems, and the interaction of the simulation system with the target protein are simulated using the GROMACS simulation software.

The GROMACS is a simulation software specialized for biological macromolecules, such as DNA, RNA, or proteins. Therefore, it will not be difficult to create the necessary files for the software for predefined macromolecules in the library of force fields. But for molecules like curcumin and fullerene, we must redefine it by adding the parameters of these molecules to the force field library.

As small molecules like curcumin, we can use automated tools to generate the parameter file for it. There are methodologies or software programs for each force field that purport to give parameters compatible with various force fields.

In the framework of this article, we chose OPLS-AA (all-atom) force field. The OPLS (Optimized Potential for Liquid Simulations) force field was developed by William L. Jorgensen and Julian Tirado-Rives at Purdue University and later at Yale University [20]. The parameters of the OPLS force field are developed and verified with experimentally obtained properties of liquid systems (density, heat of vaporization). The OPLS philosophy is based on fitting molecular mechanics (MM), the potential energy surface (PES) surfaces (parameters) to experimental data sets, which render this force field (FF) especially powerful for accurately describing condensed phase properties of small drugs.

The automated tool LigParGen (A server from the Jorgensen group to produce OPLS topologies) is chosen to get the parameter of curcumin [21–23]. The structural charge of the molecule is then optimized by DFT method.

In the case of fullerene C540, it is quite difficult to use tools that automatically generate parameter files because this molecule is very large and doesn't have any parameter file available in the library. We used the parameters of the available homologous structures of the OPLS force field library to define the carbons of the fullerene, the carbon we take the parameter of naphthalene fusion C9. The type of bond between the carbons is like Tryptophan, Tyrosine, or Phenol. We use that of phenol for the angle type and the aromatic ring for the dihedral type. We then optimized the charge of fullerene using the Tight-binding method [24].

For simulating the curcumin-encapsulated fullerene system, firstly, the initial configuration of the simulation system is optimized by 100,000 steps of the steepest descent algorithm. Then, we run an ensemble to equilibrate the system at a desired temperature and pressure (300K and 1 bar, respectively) in 8 ns.

To form the fullerene defects, the holes on the fullerene surface are created by manually removing carbon atoms in the PDB files to create new files with 5 carbon, 16 carbon, 32 carbon size holes. Next, the geometrical structures of the defective fullerene are optimized using the Tight-Binding method. New systems with 5-carbon, 16-carbon, and 32-carbon defects are then simulated following the same steps as the curcumin-encapsulated fullerene system.

From the second stage configurations, if curcumin can move out of the fullerene capsule through the defect holes, we select that structure and interact with the target protein. In case the bonds between curcumin and fullerene are too strong, we will investigate the effect of curcumin when bringing the target protein molecule close to the hole and investigate the free energy variation of the system between curcumin and fullerene the protein. Structures with proteins are also processed and simulated in the same way as the fullerene-encapsulated curcumin system.

RESULTS

The curcumin-encapsulated fullerene model

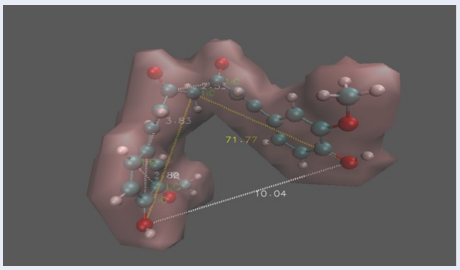

Figure 7: Visualized curcumin molecular structure using VMD.

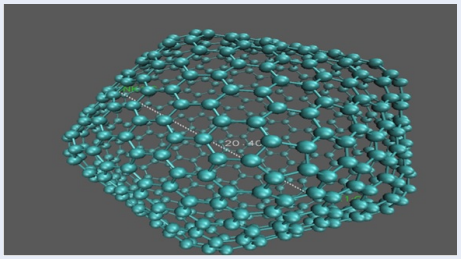

Figure 8: Visualized fullerene molecular structure using VMD.

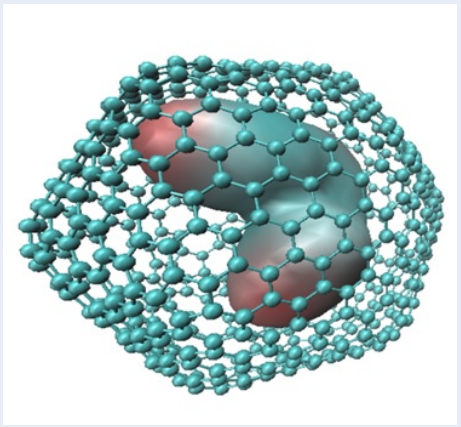

Figure 9: Visualized curcumin inside fullerene using VMD.

Fullerene defects

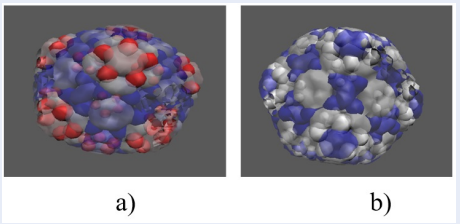

Figure 10: Fullerene molecular charge density distribution: a) According to each group with the same charge value; b) According to the group of positive and negative charges. The blue color is represented the negative charge, and white color is represented the positive charge

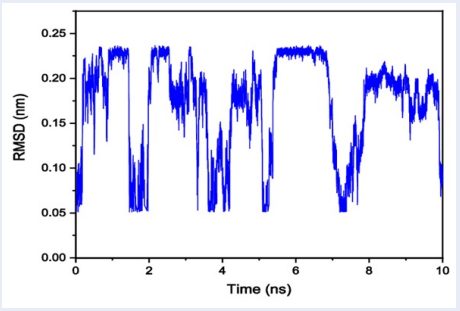

Figure 11: RMSD of the system after molecular dynamic simulation.

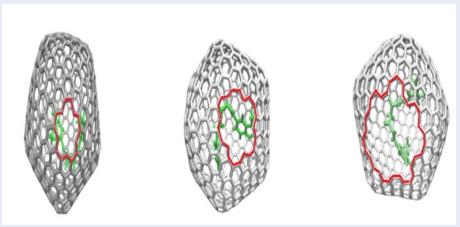

Figure 12: Molecular structure with holes in the fullerene surface.

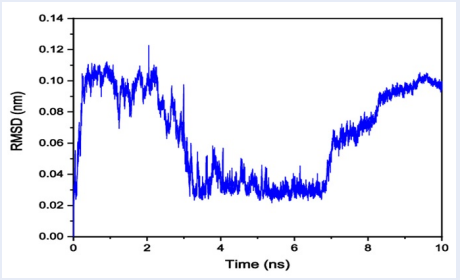

Figure 13: RMSD of 5C size fullerene defect simulation system

Table 1: Energy of the system after running molecular dynamics

Energy	Average (kJ/mol)	RMSD (nm)
Bond	34750.4	254.877
Angle	1083.71	30.638
Ryckaert-Bell.	2364.68	29.7468
Improper Dih.	5.92375	2.47288
LJ-14	1283.56	9.78819
Coulomb-14	-125.045	3.59434
LJ (SR)	61162.3	661.741
Coulomb (SR)	-80711.6	2529.22
Potential	18443.4	2571.03

Table 2: Fullerene and curcumin interaction energy

Energy	Average (kJ/mol)	RMSD (nm)
Coul-SR	0.124847	0.237061
LJ-SR	-205.551	5.45033

Table 3: Energy of the 5C size system after running the simulation.

Energy	Average (kJ/mol)	RMSD (nm)
Bond	1230.3	94.6168
Angle	1276.9	59.9649
Ryckaert-Bell.	2009.95	36.6072
Improper Dih.	5.47294	2.37605
LJ-14	5297.95	42.6237
Coulomb-14	-89.3839	3.45103
LJ (SR)	9309.14	942.624
Coulomb (SR)	-84321.8	3417.6
Potential	-65438.4	3570.16

Table 4: Energy of the 16C size system after running the simulation.

Energy	Average (kJ/mol)	RMSD (nm)
Bond	1082.42	150.476
Angle	1530.77	102.848
Ryckaert-Bell.	1942.16	43.6017
Improper Dih.	4.13165	2.00658
LJ-14	5065.33	42.1742
Coulomb-14	-103.996	3.04576
LJ (SR)	11090.8	1589.22
Coulomb (SR)	2700	5582.46
Potential	-70018.6	4345.06

Table 5: Energy of the 32c size system after running the simulation.

Energy	Average (kJ/mol)	RMSD (nm)
Bond	1148.22	108.59
Angle	1353.14	73.6681
Ryckaert-Bell.	1979.3	35.5139
Improper Dih.	4.91936	2.08934
LJ-14	4889.1	41.6641
Coulomb-14	-109.411	3.31778
LJ (SR)	10204.7	1304.42
Coulomb (SR)	-87618.8	4622.22
Potential	-68305.4	3570.16

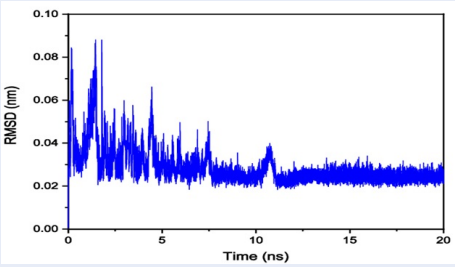

Figure 14: RMSD of 16C size fullerene defect simulation system

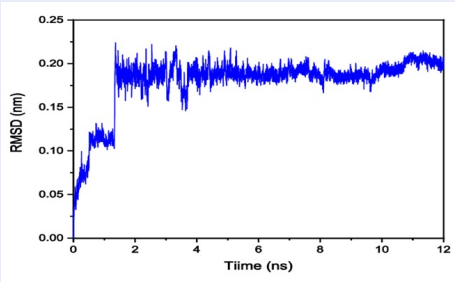

Figure 15: RMSD of 32C size fullerene defect simulation system

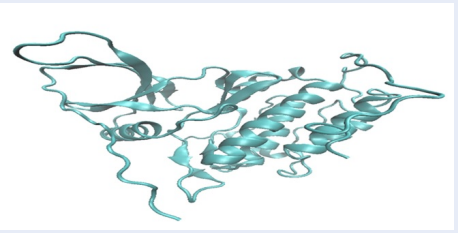

Figure 16: Structure of the epidermal growth factor receptor protein using VMD

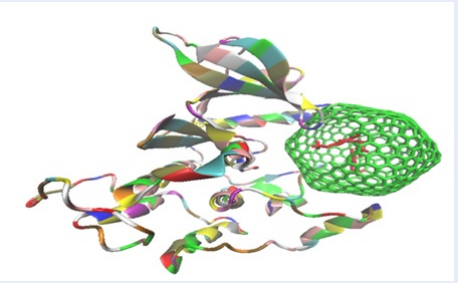

Figure 17: The simulation system includes the target protein

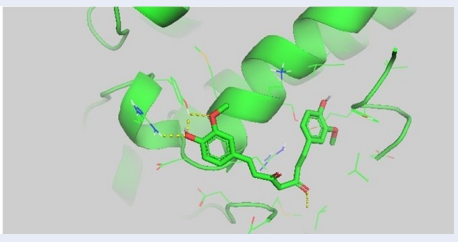

Figure 18: The position of curcumin with the highest affinity on the target

The model with a target protein

DISCUSSION

Curcumin and fullerene molecular structure

The electrostatic charge and the distance between the molecules' atoms are obtained from the optimization by using the Tight Binding method. The structural parameters of the molecules of the simulation system

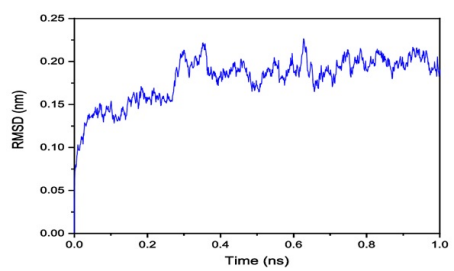

Figure 19: RMSD of protein after simulation

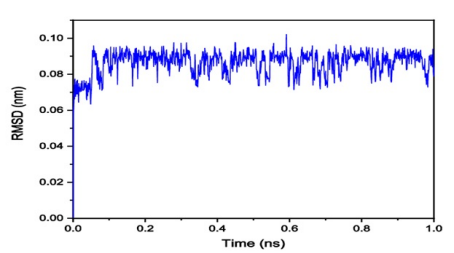

Figure 20: RMSD of curcumin after simulation

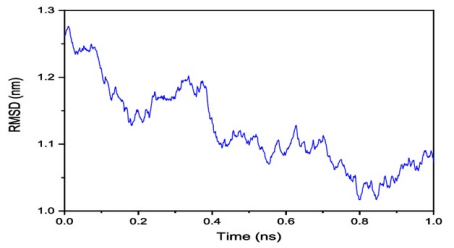

Figure 21: RMSD of curcumin and protein after simulation

are shown through visual images by VMD software.

The geometric structure of the optimized curcumin is shown in Figure 7; we find that curcumin has a symmetrical structure. For convenience, we put the curcumin molecule inside a rectangular box with the dimensions calculated. We see that the distance between the molecule's two farthest atoms (-OH) is 10.04 Å. By putting the curcumin in the rectangular box, the size of the curcumin molecule is very easy to be calculated through the parameter of this box. We estimate the volume of the curcumin molecule to be V=344 $Å^3$.

With the above curcumin size, we need a sphere diameter of more than 13.1 Å to cover all the curcumin molecules. For this size, we choose a fullerene with 540 carbons and a sphere diameter of 20.4 Å (Figure 8).

Figure 9 shows a model of a molecular system with curcumin inside a fullerene molecule. If we use a smaller size, the movement of curcumin will be very limited and will create difficulty when curcumin moves out of the fullerene envelope.

Charge distribution of fullerene

The optimization results of molecular geometry also help us obtain charge distribution values. For example, we are interested in the charge distribution of the carbon atoms of the fullerene. As shown in Figure 10, we have a total of nine charge-group distribution, which include 60 carbons per group. The reason for these charge groups is that because fullerenes have aromatic ring carbons arranged sequentially, the charge of these carbons will be periodic in the fullerene structure.

The curcumin-encapsulated fullerene model

The model of the obtained system is used to run MD molecular dynamic simulations according to the procedure of the GROMACS software. The simulation box contains 587 atoms and the TIP3P water model. We use the RMSD value to evaluate the stability of the simulation system. Looking at the simulation results in Figure 11, we see that the RMSD of the curcumin is quite large; there are periods when the system achieves stability but then quickly falls into an instability state.

The potential reason for the instability state is that the curcumin molecule is flexible inside the fullerene cage; therefore it does not form tight covalent bonds with the inner surface of the cage. In addition, according to the calculation of the molecular formula optimization method, although the fullerene is electrically neutral, some regions have a negative charge, and some regions have a positive charge. This creates strong attraction and repulsion on the curcumin atoms, and they are also charged due to the distribution of electrons.

Therefore, we can imagine that when we put the system in the simulation box, the moving water molecules will affect the curcumin molecules, making the curcumin atoms vibrate, but under the influence of the electrostatic attraction of the molecules. As a result, the fullerene cage will generate a force holding these curcumin molecules, resulting in the RMSD graph having unstable fluctuations as above.

The system's energy after running the molecular dynamics simulation is shown in Table 1. As shown in

the overview, fullerene is one of the molecules with high tension and stability at standard conditions; this leads to the potential energy of the simulated system having a positive value.

The interaction energy shown in Table 2, according to the Lenard-Jones interaction potential, has a negative value. This indicates that between these two molecules, the attractive interaction is dominant, which makes curcumin partly bind to the fullerene. Electrostatic interaction contribute to the displacement of the curcumin molecule within the fullerene, since the movement of electrons causes an uneven distribution leading to a different charge on the fullerene molecule. Therefore, the proposed model of curcumin inside a fullerene molecule can be feasible according to the obtained interaction energy values.

Fullerene defects

As the proposed system can become a curcumin delivery carrier, the interaction system does not reach a steady-state, which can be explained that the curcumin molecule tends to come out of the fullerene cage. Therefore, in this section, we create the defects on the fullerene envelope membrane like the hole sizes in Figure 12. This aims to create holes on the membrane surface to help curcumin molecule has to space to move outside.

When defects are formed, the charge distribution of the carbons changes, with the defect size of 5 carbons, some carbons with unpaired charges around the edge of the hole. The positive and negative charge groups are still interspersed. With the size of 16 carbons, there will be no carbons with equal charges, but instead, areas of negative and positive charge alternating with each other. With the size of 32 carbon , we observed the same charge distribution with 16 carbon size.

After creating defective fullerene, the simulation is conducted to evaluate the effect of the defect on curcumin behavior.

a) Hole size 5 carbons

As shown in Figure 13, during the first 10 ns, the system fluctuates sharply in the first 2 ns, from 4 ns to 7 ns, the system returns to equilibrium and then oscillates again from 8 ns to 10 ns.

Although the system shows instability, the system's tendency to become progressively more stable than in the case of no defects, we found that curcumin tends to escape at 7 ns. The energy values of the system are described in Table 3; there are some interesting points in the potential value of the system compared to the original system. We see that the potential energy in Table 3 decreased and returned to the negative value, which can be explained by the 5-carbon vacancy reducing the tension of the fullerene molecule.

b) Hole size 16 carbon

At the size of 16C vacancy, the balance was observed at 7 ns to 8 ns. For further investigation, we continue to run the system for the next 10 ns. As a result, the system reaches a stable point, like the RMSD chart in Figure 14. The obtained energy values are shown in Table 4, which shows the negative value of potential energy; at this time, the system's tension is also released due to the 16-carbon hole. Since in this situation, we still did not get the desired result of releasing curcumin from the system, we continue to investigate with a larger hole size of 32 carbons.

c) Hole size 32 carbon

With 32 carbons, the system quickly reached equilibrium after 2 ns as shown in Figure 15. The energy values obtained in Table 5 show that the tension of the fullerene molecule with the 32-carbon hole is also released. However, the curcumin still cannot escape outside the fullerene.

We recognize that when increasing the size of the defect holes on the fullerene molecule, the system tend to oscillate strongly at first and then return to equilibrium. This can be explained by the change in the charge density distribution of the fullerene and the loss of symmetry that consequently affects the movement of the curcumin molecule inside. In addition, we also conducted further simulation to study the binding properties between the fullerene and the target protein.

It is worth noting that all three sizes have similar potential energy values. All show a decrease in potential energy, so the binding of curcumin to the defective fullerene is also stable. It is very difficult for curcumin to escape from the simulation system.

The model with a target protein

The selected target protein is the epidermal cell growth factor receptor protein or EGFR for short. The molecular structure of the protein and the simulation system is visualized in Figure 16 and Figure 17.

The target protein structure shown in Figure 16 consists of 1,210 amino acids; this is a macromolecule containing nearly 5,000 atoms; the tertiary structure consists of 8 α-helices, 7 β-folded sheets, and many helix springs. The protein encoded by this gene is a transmembrane glycoprotein member of the protein kinase superfamily. This protein is a receptor for members of the epidermal growth factor family. EGFR is a cell surface protein that binds to epidermal growth factor, thus inducing receptor dimerization and tyrosine autophosphorylation leading to

cell proliferation. Mutations in this gene are associated with lung cancer. EGFR is a component of the cytokine storm that contributes to a severe form of Coronavirus Disease 2019 (COVID-19) resulting from infection with severe acute respiratory syndrome coronavirus-2 (SARS-CoV-2)[25].

The simulation system shown in Figure 17 contains a large number of atoms (5,503 atoms), so to optimize the simulation run time, we investigated which sites of the protein has a strong affinity with the curcumin, then adjusted the position closer to the hole gap of the fullerene to facilitate the interaction of curcumin.

As we know, the proteins have four structural orders, of which tertiary structures are the spatial structures. The formation of spatial structures with shapes specific to each protein affects the docking of the ligands to the target proteins. Therefore, when selecting simulation conditions, these macromolecules must be in a state of minimum energy. We conduct a simulation of protein-ligand docking using the Autodock Vina software and then conduct an information processing using Pymol software. We obtained the molecule placement close to the amino acid Arginine 977 and amino acid Tyrosine 978 in the α-helix region (Figure 18). In the next step, we adjust the coordinates of the fullerene and curcumin molecules so that these molecules are as close to amino acid positions 977 and 978 as possible.

The system is simulated by the molecular dynamics similar to the processes that we simulate the systems in the above sections, but due to a large number of atoms of the system, with limited computer resources, we conduct a simulation of 500,000 steps equivalent to 1 ns.

It is found that under the simulated conditions of the system, the target protein tends to reach a good equilibrium state, even though for 1 ns. The amino acids in the protein molecule are very flexible under simulated conditions. Still, when reaching the optimal energy states, these amino acids remain around a position and form the shapes of the protein we are interested in. In Figure 19, we saw that the bound amino acids fluctuated strongly from 0.4 ns to 0.6 ns, but then tended to equalize. However, the system needs further run with a longer time to assess protein stability. Like the three-dimensional structure of proteins, the structure of curcumin also needs to be stabilized.

As shown in Figure 20, we saw that the RMSD value of curcumin is less than 0.1 nm. During that time, curcumin has not escaped from the fullerene sphere due to the attractive forces with the membrane. Therefore, we continue to consider the RMSD plot of the curcumin and protein complexes.

Figure 21 shows the RMSD of the complex of curcumin and protein; after the molecular dynamics process, curcumin and protein did not change much after 1 ns. Since we had placed the protein very closely with curcumin, it is difficult to observe the coordinate change of this complex, so it is easy to understand the equilibrium and stable RMSD in 1 ns simulation. The graph shows that curcumin has not yet bind bound to the target protein because of the short calculation time.

CONCLUSION

A model of the curcumin molecule inside a fullerene molecule could theoretically exist. The binding energy parameters of the model are calculated. It can be concluded that the curcumin molecule has an electrostatic interaction with the charging system on the surface of the fullerene and that curcumin will move flexibly within the fullerene molecule. This is very convenient for drug molecules to move to escape outside the drug carrier system easily. The creation of holes on the surface of the curcumin molecule aims to create a space for the curcumin molecule to escape, which changes the charge density on the surface of the fullerene molecule. The curcumin molecule is observed to be unable to escape these pore-filled fullerene structures, the reason being that the binding property of curcumin to the fullerene prevents the fullerene from leaving the cage, which would prevent curcumin from escaping the membrane by the external effects, and only release when the desired goal is reached. Since the interaction of curcumin with the fullerene surface does not change the chemical nature of the curcumin molecule, it is easy to investigate the interactions of the drug molecule with its target protein using different methods of dynamic simulation. Our obtained result shows that the curcumin tends to escape when it encounters the target protein, but the calculation time is short. Therefore, the calculation with a longer computation time needs to be carried out in the future.

ACKNOWLEDGMENT

Firstly, I would like to express my sincere gratitude to Dr. Tran Thi Thu Hanh, who wholeheartedly guided, helped, spent a lot of time and effort in guiding me to complete the study.

My thanks also go to the colleagues in the computational physics laboratory, room 103B4 - Ho Chi Minh City University of Technology, for taking the time to discuss and give me valuable comments for this work.

ABBREVIATIONS

GROMACS : Groningen machine for chemical simulation: Máy Groningen để mô phỏng hóa học

RMSD: Root mean square deviation: Độ lệch căn quân phương

DFT: Density functional theory: Lý thuyết phiếm hàm mật độ

DFTB+: Density functional based Tight Binding (and more): Phiếm hàm mật độ dựa trên liên kết chặt chẽ

SR: Soft-core: Lõi mềm

LJ : Lennard-Jones

Coul.: Coulomb

PDB: Protein Data Bank: Ngân hàng dữ liệu protein

GPCR: G Protein couple receptor: Thụ thể cặp đôi protein G

EGFR: Epidermal growth factor receptor: Thụ thể yếu tố tăng trưởng biểu bì

VMD: Visual Molecular Dynamics: Trực quan hóa động lực học phân tử

Những phần dưới xin vui lòng chuyển sang tiếng Anh

XUNG ĐỘT LỢI ÍCH

Nhóm tác giả xin cam đoan rằng không có bất kỳ xung đột lợi ích nào trong công bố bài báo.

ĐÓNG GÓP CỦA TÁC GIẢ

Lê Vũ Phúc đóng góp vào việc chạy mô hình, thu thập dữ liệu, phân tích dữ liệu và viết bản thảo.

Lâm Toàn Vĩ đã đóng góp trong việc lựa chọn các phần mềm và các mô hình cần mô phỏng và chỉnh sửa dữ liệu

Trần Thị Thu Hạnh đã đóng góp việc định hướng nghiên cứu, kiểm tra dữ liệu, và chỉnh sửa bản thảo.

REFERENCES

1. Drug Delivery Systems [Internet]. Nibib.nih.gov. [cited 14 July 2021]. 2021;Available from: https://www.nibib.nih.gov/science-education/science-topics/drug-delivery-systems-getting-drugs-their-targets-controlled-manner.
2. Kroto H. C60 Buckminsterfullerene. MRS Proceedings. 1990;206:162-163;Available from: https://doi.org/10.1557/PROC-206-611.
3. Haddon R, Brus L, Raghavachari K. Electronic structure and bonding in icosahedral C60. Chemical Physics Letters. 1986;125(5-6):459-464;Available from: https://doi.org/10.1016/0009-2614(86)87079-8.
4. Kroto H. ChemInform Abstract: The Stability of Fullerenes Cn, with n = 24, 28, 32, 36, 50, 60, and 70. ChemInform. 1988;19(8):529-531;Available from: https://doi.org/10.1002/chin.198808393.
5. Kroto H, Heath J, O'Brien S, Curl R, Smalley R. C60: Buckminsterfullerene. Nature. 1985;318(6042):162-163;Available from: https://doi.org/10.1038/318162a0.
6. Bürgi H, Blanc E, Schwarzenbach D, Liu S, Lu Y, Kappes M et al. The Structure of C60: Orientational Disorder in the Low-Temperature Modification of C60. Angewandte Chemie International Edition in English. 1992;31(5):640-643;Available from: https://doi.org/10.1002/anie.199206401.
7. Hedberg K, Hedberg L, Bethune D, Brown C, Dorn H, Johnson R et al. Bond Lengths in Free Molecules of Buckminsterfullerene, C60, from Gas-Phase Electron Diffraction. Science. 1991;254(5030):410-412;PMID: 17742230. Available from: https://doi.org/10.1126/science.254.5030.410.
8. Haddon R, Brus L, Raghavachari K. Rehybridization and π-orbital alignment: the key to the existence of spheroidal carbon clusters. Chemical Physics Letters. 1986;131(3):165-169;Available from: https://doi.org/10.1016/0009-2614(86)80538-3.
9. Goodarzi S, Da Ros T, Conde J, Sefat F, Mozafari M. Fullerene: biomedical engineers get to revisit an old friend. Materials Today. 2017;20(8):460-480;Available from: https://doi.org/10.1016/j.mattod.2017.03.017.
10. Castro E, Cerón M, Garcia A, Kim Q, Etcheverry-Berríos A, Morel M et al. Correction: A new family of fullerene derivatives: fullerene-curcumin conjugates for biological and photovoltaic applications. RSC Advances. 2019;9(5):2379-2379;Available from: https://doi.org/10.1039/C9RA90002K.
11. Tran T, Le M, Tran T, Tran T, Thai K. Design of Curcumin and Flavonoid Derivatives with Acetylcholinesterase and Beta-Secretase Inhibitory Activities Using in Silico Approaches. Molecules. 2020;25(16):3644;PMID: 32785161. Available from: https://doi.org/10.3390/molecules25163644.
12. Thong N, Dao D, Ngo T, Huyen T, Nam P. Antioxidant activities of [60]fullerene derivatives from chalcone, flavone and flavanone: A ONIOM approach via H-atom and electron transfer mechanism. Chemical Physics Letters. 2016;652:56-61;Available from: https://doi.org/10.1016/j.cplett.2016.04.036.
13. Golonko A, Lewandowska H, Świsłocka R, Jasińska U, Priebe W, Lewandowski W. Curcumin as tyrosine kinase inhibitor in cancer treatment. European Journal of Medicinal Chemistry. 2019;181:111512;PMID: 31404861. Available from: https://doi.org/10.1016/j.ejmech.2019.07.015.
14. Wang P, Yan G, Zhu X, Du Y, Chen D, Zhang J. Heterofullerene MC59 (M = B, Si, Al) as Potential Carriers for Hydroxyurea Drug Delivery. Nanomaterials. 2021;11(1):115;PMID: 33430313. Available from: https://doi.org/10.3390/nano11010115.
15. Carroll R, Benya R, Turgeon D, Vareed S, Neuman M, Rodriguez L et al. Phase IIa Clinical Trial of Curcumin for the Prevention of Colorectal Neoplasia. Cancer Prevention Research. 2011;4(3):354-364;PMID: 21372035. Available from: https://doi.org/10.1158/1940-6207.CAPR-10-0098.
16. Lao C, Ruffin M, Normolle D, Heath D, Murray S, Bailey J et al. Dose escalation of a curcuminoid formulation. BMC Complementary and Alternative Medicine. 2006;6(1);PMID: 16545122. Available from: https://doi.org/10.1186/1472-6882-6-10.
17. Sharma R, Euden S, Platton S, Cooke D, Shafayat A, Hewitt H et al. Phase I Clinical Trial of Oral Curcumin. Clinical Cancer Research. 2004;10(20):6847-6854;PMID: 15501961. Available from: https://doi.org/10.1158/1078-0432.CCR-04-0744.
18. Curcumin [Internet]. Pubchem.ncbi.nlm.nih.gov. 2021 [cited 23 August 2021];Available from: https://pubchem.ncbi.nlm.nih.gov/compound/Curcumin.
19. Bank R. RCSB PDB - 4I23: Crystal structure of the wild-type EGFR kinase domain in complex with dacomitinib (soaked) [Internet]. Rcsb.org. 2021 [cited 23 August 2021];Available from: https://www.rcsb.org/structure/4I23.
20. Vo VH. Simulation in physic. 1st ed. Ho Chi Minh: Ho Chi Minh National University. 2016;.
21. Jorgensen W, Tirado-Rives J. Potential energy functions for atomic-level simulations of water and organic and biomolecular systems. Proceedings of the National Academy of Sciences. 2005;102(19):6665-6670;PMID: 15870211. Available from: https://doi.org/10.1073/pnas.0408037102.
22. Dodda L, Vilseck J, Tirado-Rives J, Jorgensen W. 1.14*CM1A-LBCC: Localized Bond-Charge Corrected CM1A Charges for Condensed-Phase Simulations. The Journal of Physical Chemistry B. 2017;121(15):3864-3870;PMID: 28224794. Available from: https://doi.org/10.1021/acs.jpcb.7b00272.

23. Dodda L, Cabeza de Vaca I, Tirado-Rives J, Jorgensen W. LigParGen web server: an automatic OPLS-AA parameter generator for organic ligands. Nucleic Acids Research. 2017;45(W1):W331-W336;PMID: 28444340. Available from: https://doi.org/10.1093/nar/gkx312.
24. Fürst JA, et al. Electronic transport properties of fullerene functionalized carbon nanotubes: Ab initio and tight-binding calculations. Physical Review B, 2009, 80(3);Available from: https://doi.org/10.1103/PhysRevB.80.035427.
25. EGFR epidermal growth factor receptor [Homo sapiens (human)] - Gene - NCBI [Internet]. Ncbi.nlm.nih.gov. 2021 [cited 17 October 2021];Available from: https://www.ncbi.nlm.nih.gov/gene/1956.

Tạp chí Phát triển Khoa học và Công nghệ
Đại học Quốc gia Tp. Hồ Chí Minh

Tạp chí Phát triển Khoa học và Công nghệ
ISSN: 1859-0128
Hình thức xuất bản: In và trực tuyến
Hình thức truy cập: Truy cập mở (Open Access)
Ngôn ngữ bài báo: Tiếng Anh
Tỉ lệ chấp nhận đăng 2021: 72%
Phí xuất bản: Miễn phí
Thời gian phản biện: 43 ngày
Lập chỉ mục (Indexed): Google Scholar, Scilit

SCAN ME

Tạp chí Phát triển Khoa học và Công nghệ - Khoa học Tự nhiên
ISSN: 2588-106X
Hình thức xuất bản: In & trực tuyến
Hình thức truy cập: Truy cập mở
Ngôn ngữ bài báo: Tiếng Việt
Tỉ lệ chấp nhận đăng 2021: 75%
Phí xuất bản: Miễn phí
Thời gian phản biện: 30-45 ngày
Lập chỉ mục (Indexed): Google Scholar, Scilit

SCAN ME

Tạp chí Phát triển Khoa học và Công nghệ - Kĩ thuật và Công nghệ
ISSN: 2615-9872
Hình thức xuất bản: In & trực tuyến
Hình thức truy cập: Truy cập mở
Ngôn ngữ bài báo: Tiếng Việt
Tỉ lệ chấp nhận đăng 2021: 61%
Phí xuất bản: Miễn phí
Thời gian phản biện: 50 ngày
Lập chỉ mục (Indexed): Google Scholar, Scilit

SCAN ME

Tạp chí Phát triển Khoa học và Công nghệ - Kinh tế-Luật và Quản lý
ISSN: 2588-1051
Hình thức xuất bản: In & trực tuyến
Hình thức truy cập: Truy cập mở
Ngôn ngữ bài báo: Tiếng Việt
Tỉ lệ chấp nhận đăng 2021: 65%
Phí xuất bản: Miễn phí
Thời gian phản biện: 45 ngày
Lập chỉ mục (Indexed): Google Scholar, Scilit

SCAN ME

Tạp chí Phát triển Khoa học và Công nghệ - Khoa học Xã hội và Nhân văn
ISSN: 2588-1043
Hình thức xuất bản: In & trực tuyến
Hình thức truy cập: Truy cập mở
Ngôn ngữ bài báo: Tiếng Việt
Tỉ lệ chấp nhận đăng 2021: 62%
Phí xuất bản: Miễn thu phí đối với tác giả là CBVC của ĐHKHXHNV, ĐHQG-HCM; Tác giả khác: 500.000 VNĐ/bài
Thời gian phản biện: 75 ngày
Lập chỉ mục (Indexed): Google Scholar, Scilit

SCAN ME

Tạp chí Phát triển Khoa học và Công nghệ - Khoa học Trái đất và Môi trường
ISSN: **2588-1078**
Hình thức xuất bản: In & trực tuyến
Hình thức truy cập: Truy cập mở
Ngôn ngữ bài báo: Tiếng Việt và tiếng Anh
Tỉ lệ chấp nhận đăng 2021: 87%
Phí xuất bản: liên hệ tòa soạn
Thời gian phản biện: 45 ngày
Lập chỉ mục (Indexed): Google Scholar, Scilit

SCAN ME

Tạp chí Phát triển Khoa học và Công nghệ - Khoa học Sức khỏe
ISSN: 2734-9446
Hình thức xuất bản: In & trực tuyến
Hình thức truy cập: Truy cập mở
Ngôn ngữ bài báo: Tiếng Việt
Tỉ lệ chấp nhận đăng 2021: 70%
Phí xuất bản: Miễn phí
Thời gian phản biện: 30 ngày
Lập chỉ mục (Indexed): Google Scholar, Scilit

SCAN ME

Tạp chí Phát triển Khoa học và Công nghệ, Đại học Quốc gia Tp.HCM
25 năm xuất bản học thuật (1997-2022)
Tòa soạn: Nhà điều hành Đại học Quốc gia Tp.HCM, P. Linh Trung, TP. Thủ Đức, TP. HCM
Email: stdj@vnuhcm.edu.vn; tcptkhcn@vnuhcm.edu.vn; Website: *http://www.scienceandtechnology.com.vn*